

Visit [Nature news](#) for the latest coverage and read [Springer Nature's statement on the Ukraine conflict](#)



Native Mass Spectrometry Analysis of Affinity-Captured Endogenous Yeast RNA Exosome Complexes

The Eukaryotic RNA Exosome pp 357-382 | Cite as

Protocol

First Online: 26 November 2019



Citations Mentions Downloads

Part of the [Methods in Molecular Biology](#) book series (MIMB, volume 2062)

Abstract

Native mass spectrometry (MS) enables direct mass measurement of intact protein assemblies generating relevant subunit composition and stoichiometry information. Combined with cross-linking and structural data, native MS-derived information is crucial for elucidating the architecture of macromolecular assemblies by integrative structural methods. The exosome complex from budding yeast was among the first endogenous protein complexes to be affinity isolated and subsequently characterized by this technique, providing improved understanding of its composition and structure. We present a protocol that couples efficient affinity capture of yeast exosome complexes and sensitive native MS analysis, including rapid affinity isolation of the endogenous exosome complex from cryolysed yeast cells, elution in nondenaturing conditions by protease cleavage, depletion of the protease, buffer exchange, and native MS measurements using an Orbitrap-based instrument (Exactive Plus EMR).

Key words

Native mass spectrometry Endogenous protein assemblies Exosome complex Affinity capture Exactive Plus EMR

Access to this content is enabled by [The Rockefeller University](#)

[Download](#) protocol PDF

1 Introduction

Most cellular processes involve the concerted actions of biological macromolecules that assemble into working modules [1]. Structural and functional elucidation of such assemblies requires information on subunit composition, stoichiometry, and connectivity obtained from multiple analytical and biophysical techniques [2, 3, 4, 5]. One direct approach is native mass spectrometry (MS), wherein critical noncovalent interactions are maintained during sample analysis enabling detection and mass measurement of intact assemblies and parts thereof [5, 6, 7, 8, 9]. With the measured intact mass of a protein assembly and the masses of its constituent subunits, the subunit stoichiometry—the number of copies of each subunit per assembly—can be deduced. Native MS has been applied with remarkable success in the structural and biochemical investigation of many protein assemblies [10, 11, 12] although many of them have been reconstituted from overexpression in recombinant systems. It is of primary importance to robustly extend the application of native MS to the study of endogenous protein assemblies—those directly isolated from their natural cellular milieu at specific functional and oligomeric states. In addition, the characterization of such endogenous protein

assemblies reveals relevant posttranslational modifications and molecular associations (e.g., binding of native cofactors or ligands) that might otherwise be lost from outsourcing protein production to heterologous systems (see also Chapters [13](https://doi.org/10.1007/978-1-4939-9822-7_13) (https://doi.org/10.1007/978-1-4939-9822-7_13) and [18](https://doi.org/10.1007/978-1-4939-9822-7_18) (https://doi.org/10.1007/978-1-4939-9822-7_18)).

The availability of large libraries of affinity-tagged strains and advances in genomic modification strategies have enabled unprecedented opportunities for the isolation of endogenous protein assemblies. For instance, high-throughput and global analysis of protein assemblies from tandem affinity purification (TAP) libraries in budding yeast has generated an extensive protein-protein interaction network revealing the modular and hierarchical organization of proteins within a eukaryotic cell [[13](#), [14](#)]. The exosome complex, an essential protein complex involved in RNA processing [[15](#), [16](#)], was among the first protein assemblies from budding yeast that was affinity-isolated by the TAP approach and subsequently characterized by native MS [[17](#), [18](#)] (see also Chapter [15](#) (https://doi.org/10.1007/978-1-4939-9822-7_15)). These studies verified that the yeast exosome core complex, designated here as Exo-10, is composed of ten subunits with one copy each of Csl4p, Mtr3p, Rrp4p, Rrp40p, Rrp41p, Rrp42p, Rrp43p, Rrp45p, and Rrp46p together with the catalytic Dis3p subunit. The organization and elements of intersubunit connectivity within Exo-10 were also uncovered from systematic in-solution and gas-phase dissociation experiments that were part of the native MS analysis workflow used [[17](#), [18](#)]. In addition, affinity isolation of compartment-specific exosome complexes confirmed distinctions in nuclear and cytoplasmic protein partners, yielding insights into distinct functions of the exosome [[19](#), [20](#)]. In these studies, sample preparation involved mechanical cell lysis using glass beads followed by multiple affinity purification and chromatographic steps prior to native MS. Prolonged handling may lead to dissociation of complexes and extensive sample loss. When procedural improvements can increase the yield of the target complex, a concomitant reduction in the burden of sample quantity is realized.

To address the need for an efficient and robust native MS pipeline, we present a protocol that couples rapid, high-yield affinity capture of the exosome via Csl4p-TAP with sensitive native MS analysis [[21](#)]. Flash-freezing cells in liquid nitrogen and subsequent mechanical cryolysis preserves noncovalent associations within the cellular milieu and minimizes proteolytic degradation of the target protein complex. In addition, the resulting cryomilled powder can be stored in -80 °C and portions can be weighed depending on the scale of the experiment allowing flexibility in the experimental design. For affinity capture, the TAP tag consists of the protein A tag from *Staphylococcus aureus* (SpA) and the calmodulin-binding protein (CBP) tag; a cleavage site for tobacco etch virus (TEV) protease is engineered between the two affinity handles [[22](#), [23](#)]. A single-step affinity capture via the SpA handle using IgG-conjugated magnetic beads is sufficient to efficiently isolate the endogenous TAP-tagged exosome complex from cell extracts [[21](#), [24](#), [25](#), [26](#), [27](#)]. IgG-conjugated magnetic beads facilitate rapid enrichment and protease elution of the captured protein complexes into small volumes (typically 10–20 μ L) keeping the sample at concentrations (several hundreds of nM) sufficiently high for native MS analysis. After elution, the 27-kDa TEV protease, which is added in excess for on-bead protease cleavage, can be efficiently removed using a centrifugal filter with a 100 kDa molecular weight cutoff (MWCO). Rapid buffer exchange into a nondenaturing and electrospray-compatible solution of volatile salt such as ammonium acetate is performed using spin columns. A small amount of Tween-20 (0.001–0.01% v/v), a nonionic detergent and common passivating agent, is added in the buffer exchange solution to enable maximum sample recovery without observable issues in subsequent MS analysis [[21](#)]. Native MS measurements are performed using the Exactive Plus EMR, an Orbitrap-based instrument that is modified for transmission and detection of macromolecular assemblies with exceptional sensitivity and high resolving power [[28](#)]. Overall, the workflow described here takes 2–3 h from the resuspension of cryomilled cell powder to a native MS-ready sample minimizing the time that the complexes spend out of their native environment and increasing experimental throughput.

2 Materials

2.1 Cryolysis of Yeast Cells

1. At least 4 L yeast cell culture: for this protocol, we use the Csl4p-TAP yeast strain (Sc BY4741 cell line from ref. [29](#)).
2. Refrigerated centrifuge and rotor for pelleting large cell volumes.
3. Refrigerated centrifuge and rotor for 50-mL tubes.
4. 50-mL polypropylene Falcon tubes.
5. Liquid nitrogen.
6. Cryoprotective gloves.
7. Styrofoam box.
8. 12% w/v polyvinylpyrrolidone (PVP), an extracellular cryoprotectant. Dissolve 1.2 g PVP in 10 mL ddH₂O.
9. 200 mM HEPES, pH 7.4: For 10 mL, dissolve 476.6 mg HEPES in 9 mL ddH₂O. Adjust pH by adding 1 M KOH. Add ddH₂O to 10 mL.
10. Yeast storage buffer (YSB): 20 mM HEPES pH 7.5, 1.2% PVP. For 10 mL, combine 1 mL 12% w/v PVP, 1 mL 200 mM HEPES pH 7.4 and 8 mL ddH₂O.
11. 25-mL or 50-mL syringe.

12. Retsch Planetary Ball Mill PM100.
13. Retsch cryomilling jar assembly: stainless steel jar (50-mL or 125-mL), lid, and 20-mm balls.
14. Tongs.
15. Spatula.

2.2 Antibody Conjugation of Magnetic Beads

1. Vacuum aspirator.
2. Dynabeads M-270 Epoxy (Thermo Fisher Scientific).
3. Magnetic separator for microcentrifuge tubes (Thermo Fisher Scientific).
4. 2-mL round-bottom tubes.
5. Tube shaker for microfuge tubes.
6. IgG purified from pooled rabbit serum (e.g., from MP Biomedicals): reconstitute lyophilized powder in ddH₂O to a final concentration of 10–20 µg/µL. Aliquot and store in –80 °C.
7. 0.1 M sodium phosphate, pH 7.4: For 1 L, dissolve 2.6 g NaH₂PO₄·H₂O and 21.7 g Na₂HPO₄·7H₂O in 1 L. Check the pH. Filter and store at RT.
8. 3 M ammonium sulfate: For 50 mL, dissolve 19.8 g (NH₄)₂SO₄ in 50 mL of 0.1 M sodium phosphate buffer, pH 7.4. Filter and store at RT.
9. Rotating wheel in an incubator (temperature set to 30 °C).
10. 0.1 M glycine–HCl pH 2.5.
11. 10 mM Tris–HCl pH 8.8.
12. 0.1 M trimethylamine (TEA)—make fresh. For 1 mL, mix 14 µL of TEA with 986 µL ddH₂O.
13. Phosphate-buffered saline (PBS).
14. PBS with 0.5% (w/v) Triton X-100.
15. PBS with 50% glycerol.

2.3 Affinity Capture of Endogenous Yeast Exosome Complex

1. Cryomilled cell powder (from Subheading [3.1](#) of this protocol).
2. Conjugated IgG Dynabeads stock: 0.1 mg/µL (from Subheading [3.2](#) of this protocol).
3. cComplete™ EDTA-free Protease Inhibitor Cocktail (Roche).
4. Magnetic separator for microcentrifuge tubes (Thermo Fisher Scientific).
5. Affinity capture (AC) buffer: 20 mM HEPES pH 7.4, 150 mM NaCl, 1.5 mM MgCl₂, 0.15% v/v Nonidet P40. For 10 mL, combine: 1 mL 200 mM HEPES pH 7.4., 0.75 mL 20 mM MgCl₂, 0.3 mL 5 M NaCl, 150 µL 10% NP-40, and 7.8 mL deionized H₂O. Keep AC buffer at room temperature.
6. 5-mL round-bottom polypropylene tubes.
7. Vacuum aspirator.

2.4 Elution by Protease Cleavage

1. AcTEV protease (Invitrogen), concentration is 1 µg/µL.
2. TEV protease buffer: 50 mM Tris pH 8, 500 µM EDTA, 1 mM DTT, 100 mM NaCl, 0.05% Tween-20. For 10 mL, combine: 0.5 mL of 1 M Tris pH 8, 50 µL of 100 mM EDTA, 50 µL of 0.2 M DTT, 0.2 mL of 5 M NaCl, 50 µL of 10% Tween-20, and 9.2 mL deionized H₂O. Keep TEV buffer on ice.

2.5 Removal of Protease and Buffer Exchange

1. Centrifugal filters: Amicon Ultra-0.5 Centrifugal Filter Unit with Ultracel-100 membrane, 100 kDa MWCO (EMD Millipore).
2. Refrigerated microcentrifuge.
3. 5 M Ammonium acetate stock solution: Dissolve 3.85 g of solid ammonium acetate (>98% pure) in a final volume of 10 mL using HPLC-grade H₂O. Filter (0.22 µm filter unit) and store at 4 °C for up to 3 months.
4. 10% Tween-20, Surfact-Amps Detergent Solution (Thermo Fisher Scientific). Store 50–100 µL aliquots in –20 °C.
5. 1.5 M ammonium hydroxide: For 1 mL, combine 50 µL HPLC-grade concentrated ammonium hydroxide with 450 µL HPLC-grade H₂O. Vortex to mix. Store at 4 °C for up to 3 months.
6. Buffer exchange (BE) solution: 400 mM ammonium acetate, pH 7.5, 0.01% Tween-20. For 1 mL, combine: 913 µL HPLC H₂O, 80 µL 5 M ammonium acetate stock, 6 µL 1.5 M ammonium hydroxide, and 1 µL 10% Tween-20. Vortex to mix. Check the pH. Prepare fresh each time.
7. Zeba Micro Spin Desalting Columns, prepacked 75 µL resin bed volume, 7 kDa or 40 kDa MWCO (Thermo Fisher Scientific).
8. Capless 2.0 mL spin column collection tubes (can be washed and reused): from Bio-Rad or made in-house by removing the caps of 2-mL microfuge tubes.

2.6 Preparation of Gold-Coated Emitters

1. Sutter Tip Puller Model P-2000.
2. Quartz tubing without filament: 1.0 mm O.D., 0.70 mm I.D., 10 cm length (Sutter Instrument).
3. Edwards S150 Sputter Coater.
4. Watch glass, 7.5 cm diameter.
5. Double-sided foam mounting tape, ~2 mm thick (Scotch).
6. Scissors.
7. Tweezers.
8. Petri dish or nanospray tip boxes for storing emitters.

2.7 Native MS Analysis

1. Exactive Plus with Extended Mass Range (EMR) Mass Spectrometer (Thermo Fisher Scientific) (*see Note 1*).
2. Nanospray off-line kit for the EMR (nanospray source head for the Nanoflex Ion source and spare parts for off-line analysis) (Thermo Fisher Scientific).
3. Handheld multifunctional vacuum pump (*see Note 2*).
4. Tweezers.
5. Ceramic glass cutter.
6. Benchtop minicentrifuge.
7. Cesium iodide, analytical standard (>99.999% trace metal basis).
8. 0.5–20 µL gel-loading tips.
9. Gold-coated emitter tips (prepared from Subheading 3.4 of this protocol).
10. Spin-adaptor assembly composed of a SwageLok (1/16th tubing male-to-male conical) with a rubber ferrule inside (from the nanospray off-line kit) to hold the emitter into place (Fig. 1a).

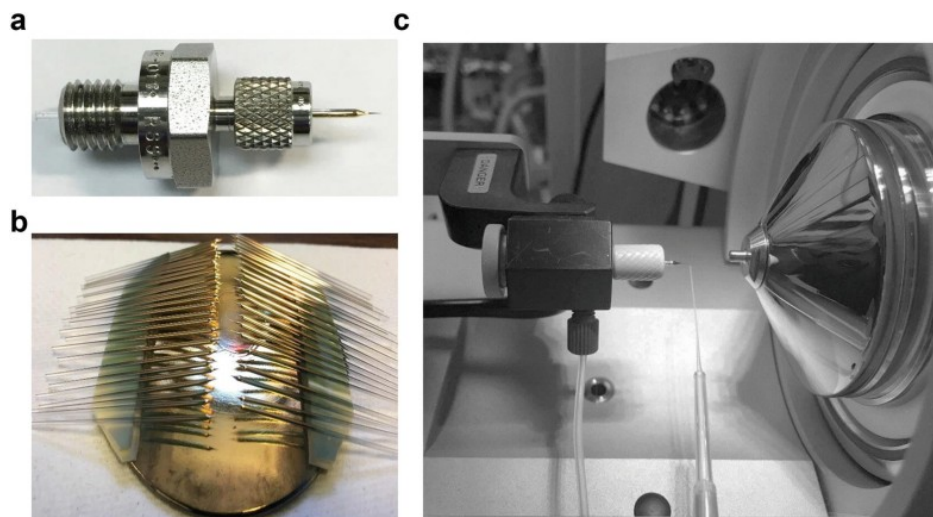


Fig. 1

Preparation of gold-coated emitters for nano-electrospray native MS. **(a)** Spin adapter assembly with a loaded emitter. **(b)** Arrangement of pulled emitters on an inverted watch glass for the sputter-coating procedure. **(c)** Initiation of sample electro-spray by lightly touching or grazing the emitter's tip with a fine, gel-loading pipette tip

3 Methods

3.1 Cryomilling of Yeast Cells

This section involves harvesting, flash-freezing and cryolysis of yeast cells that is optimized for generating micron-scale cell powder enabling efficient lysate resuspension and affinity capture [24, 26, 30]. It is crucial to follow the prescribed safety procedures and take extreme care when handling liquid nitrogen. Protective lab clothing and cryoprotective gloves must be used at all times during cryomilling. Consult the National Center for Dynamic Interactive Research website (www.ncdir.org/public-resources/protocols) (<http://www.ncdir.org/public-resources/protocols>) for videos and further updates on cryogenic disruption of yeast cells.

1. Grow the yeast cell culture to a density of at least 3.0×10^7 cells/mL. Spin cultures down at $4000 \times g$ for 10 min at 4 °C. Discard the supernatant.
2. Gently resuspend the cell pellet in 25 mL of ice-cold ddH₂O. Pool the mixtures into 50-mL Falcon tubes and spin down at $2600 \times g$ for 5 min at 4 °C.
3. Note the volume of the cell pellet and resuspend in an equal volume of YSB. Spin down at $2600 \times g$ for 15 min. Decant the supernatant. To fully remove all the liquid, spin down again at $2600 \times g$ for 15 min and aspirate all the liquid from the pellet.
4. Fill a clean Styrofoam box with liquid nitrogen. Submerge a conical tube rack for 50-mL Falcon tube into the bath. Prepare a 50-mL Falcon tube. Poke its cap with a syringe needle to form tiny holes. Unscrew the cap and place the Falcon tube into the tube rack inside the cooling bath. Fill the tube with liquid nitrogen.
5. With a spatula, transfer the cell paste into a 20-mL or 50-mL syringe depending on the cell pellet volume.
6. Gently press the plunger and extrude the cell slurry directly into the cryocooled 50-mL Falcon tube forming frozen strings of cell paste or “noodles.”
7. When the tube is full, screw on the cap with holes and pour off the excess liquid nitrogen. Store the frozen noodles at -80 °C until cryomilling.
8. For the cryomilling process, set-up a liquid nitrogen station beside the planetary ball mill. Precool the components for cryomilling (stainless steel jar, lid, and balls) by immersion in liquid nitrogen. Once the vigorous boiling in the bath ceases, take out the pre-cooled milling jar and add the frozen yeast noodles

- (<20 mL of noodles/50-mL jar or 20–50 mL of noodles/125-mL jar). Place three balls to the 50-mL jar or 7–11 balls to the 125-mL jar.
9. Replace the lid of the milling jar. Weigh the complete jar assembly and adjust the corresponding counterbalance weight. Ensure all liquid nitrogen has evaporated off inside the jar before milling to prevent the buildup of excess pressure.
 10. Place the assembled milling jar in the planetary ball mill and clamp down as per manufacturers' instructions. Ensure that the jar is securely clamped to prevent accidents or damages.
 11. Setup the milling cycle. For the 125-mL jar, set 400 rpm rotation speed, 3 min grinding time, and 1 min interval for reverse rotation with no breaks between rotations. For the 50-mL jar, set 500 rpm speed with the same timing parameters as the 125-mL jar.
 12. Start the cryomilling sequence. You must hear the balls rattling around inside the jar. If there is no rattling sound, wait for the cycle to finish, unclamp the jar, and add or remove balls (see **Note 3**).
 13. When the milling sequence is complete, unclamp and place the milling jar in the liquid nitrogen bath. Do not completely submerge the jar to prevent the liquid nitrogen from entering the jar. Using tongs and a 50-mL Falcon tube, pour liquid nitrogen on the lid to cool the unsubmerged portion of the jar. Once the whole assembly is fully cooled, reclamp the jar as before and start another cycle.
 14. Perform eight to ten milling cycles (repeat **steps 11–13**).
 15. After the eighth cycle, open the jar, place a small amount of powder into a microscope slide and examine under a microscope. Assess the grinding efficiency by comparing the amount of intact yeast cells relative to the amount of milled powder (amorphous, powdery background).
 16. If there is less than 20% intact cells, proceed to **step 17**. Otherwise, continue with the cryomilling. Assess grinding efficiency (**step 15**) after every subsequent cycle.
 17. If the cryomilling is >80% complete, remove the steel balls and transfer the yeast powder into a precooled, preweighed 50-mL Falcon tube using a prechilled metal spatula. Work quickly to avoid thawing the cell powder. Record the mass of the cryomilled cell powder.
 18. Store the cell powder until needed at -80°C .

3.2 Antibody Conjugation of Magnetic Beads

This protocol is adopted from ref. **31** with some modifications and is tailored for conjugation of 50 mg magnetic beads, which is sufficient for several native MS experiments.

1. Weigh 50 mg of magnetic beads in a 2-mL microfuge tube.
2. Wash beads with 1 mL 0.1 M sodium phosphate buffer, pH 7.4. Vortex for 30 s and mix on a tube shaker for 15 min at RT. Place the tube on a magnet and aspirate the wash liquid. Repeat the wash step once.
3. The ideal conjugation volume for 50 mg beads is 1 mL. On a separate tube, mix an equivalent of 500 μg of IgG stock (10 $\mu\text{g}/\text{mg}$ bead) and 0.1 M sodium phosphate pH 7.4 to make a volume of 0.5 mL (see **Note 4**). Add 0.5 mL of 3 M ammonium acetate. Transfer into the washed magnetic beads and mix well.
4. Wrap the 2-mL tube containing the conjugation mixture with Parafilm and place on a rotating platform at 30°C overnight for 20–24 h.
5. On the next day, wash beads sequentially with 1 mL each of the following:
 - (a) 0.1 M sodium phosphate pH 7.4,
 - (b) 0.1 M Glycine-HCl pH 2.5—add, mix well and aspirate as quickly as possible. Prolonged incubation in highly acidic conditions may lead to IgG denaturation,
 - (c) 10 mM Tris-HCl pH 8.8,
 - (d) 0.1 M triethylamine solution—add, mix well and aspirate as quickly as possible. Prolonged exposure to highly alkaline conditions may lead to IgG denaturation,
 - (e) Five washes with PBS (transfer beads to a new, clean tube during the second wash).
 - (f) PBS with 0.5% TritonX-100 for 15 min with rotation in the fridge,
 - (g) PBS (transfer beads to another tube before aspirating the wash liquid).
6. Resuspend beads in 450 μL PBS with 50% glycerol. Measure final volume after mixing (final concentration: ~ 0.1 mg/ μL). Store at -20°C .

3.3 Sample Preparation for Native MS Analysis

3.3.1 Affinity Capture of the Exosome Assembly from Budding Yeast

The protocol adopts a highly optimized affinity capture methodology for maximum recovery of the endogenous protein assembly of interest [21, 24, 25, 26, 27]. About 0.5 g of cryomilled cell powder (~0.25 L of yeast culture) is typically sufficient material for obtaining good native MS signals for the intact yeast Exo-10 assembly.

1. Weigh 0.5 g of cryomilled yeast powder in a 15-mL Falcon tube with a prechilled spatula.
2. Let the tube containing the frozen powder stand at room temperature for 1 min.
3. Add 2.25 mL AC buffer (kept at room temperature) with 50 μ L of 50 \times EDTA-free protease inhibitor cocktail (see **Note 5**). Vortex for 30 s to completely resuspend the cell powder. Keep the resuspended lysate on ice.
4. Distribute the cell lysate into three 1.5-mL microfuge tubes (~0.75 mL of lysate each). Clarify the lysate by spinning in a refrigerated benchtop centrifuge at maximum setting (16,000 $\times g$) for 10 min at 4 $^{\circ}$ C.
5. While the cell lysate is being centrifuged, take 40 μ L of the IgG-conjugated magnetic beads (see **Note 6**). Wash the beads twice with 500 μ L AC buffer by gently pipetting the beads up and down. Resuspend equilibrated beads in 50 μ L AC buffer and keep on ice.
6. When the centrifugation of lysate is finished, carefully collect the supernatant (clarified lysate) to a 5-mL tube. Discard the pellet.
7. Add the prewashed beads from **step 5** to the cleared lysate, cap the tube and incubate with rotation at 4 $^{\circ}$ C for 30 min (see **Note 7**).
8. Place the lysate-bead mixture on a magnet and aspirate the supernatant. Add 500 μ L AC buffer to collect beads then transfer to a clean 1.5-mL microfuge tube.
9. Wash the beads twice with 500 μ L AC buffer.

3.3.2 Nondenaturing Elution by Protease Cleavage

Nondenaturing, on-bead elution can be performed either by incubation with a competitive peptide or by protease cleavage (see **Note 8**). This section describes elution by TEV protease release as the TAP tag contains an engineered TEV cleavage site. The TEV protease is the 27-kDa catalytic domain of a viral cysteine protease that specifically recognizes the heptapeptide sequence ENLYFQG, cleaving between Gln and Gly [32, 33, 34]. It is a robust protease that is active at 4 $^{\circ}$ C. We found that ~1 μ g of TEV protease per 1 g of cryogridate was sufficient to yield full cleavage of bead-bound, affinity-tagged protein complex at 4 $^{\circ}$ C [21] (see **Note 9**). For 0.5 g starting cell powder, 0.5 μ g TEV protease is used.

1. Wash the magnetic beads with bound protein complexes twice with 500 μ L TEV buffer.
2. After the final wash, briefly spin the beads in a tabletop minicentrifuge. Place on a magnet and remove as much liquid as possible.
3. In a separate tube, mix 0.5 μ L AcTEV protease stock with 20 μ L TEV buffer (final concentration: 25 ng/ μ L AcTEV, assuming 1 μ g/ μ L of protease stock).
4. Add the protease solution into the beads. Mix the slurry by slowly pipetting up and down.
5. Incubate with rotation or gentle agitation at 4 $^{\circ}$ C for 30–60 min.

3.3.3 Protease Removal

The protease must be depleted prior to native MS analysis to minimize interference and dominant peak signals from the protease. In this protocol, we use a 0.5 mL centrifugal filter with a 100 kDa MWCO to rapidly remove the 27-kDa TEV protease with minimal sample loss [21] (see **Note 10**).

All centrifuge spins are performed at 13,400 $\times g$, 4 $^{\circ}$ C unless otherwise indicated.

1. While the sample is incubating with the protease, load 500 μ L HPLC-grade H₂O on the centrifugal filter. Centrifuge for 5 min.
2. Load filter with 500 μ L TEV buffer. Spin for 5 min. Repeat this step. Afterwards, the membrane filter should have been equilibrated and the filter is free of storage stabilizers such as glycerol, which can significantly interfere with MS analysis. Keep the membrane wet at all times. Leave some buffer on the filter until the sample is ready.
3. After the protease incubation step, briefly spin the bead mixture on a tabletop centrifuge to collect all the liquid. Place the tube on a magnet. Collect the eluate (~20 μ L) and transfer to a new 0.5-mL microfuge tube. Take an aliquot (10% of eluate volume) for SDS-PAGE analysis. Also, save the magnetic beads for sample analysis later (Subheading 3.6).

4. Wash the beads with 10–30 μL TEV buffer. Collect the wash and pool the volumes with the initial eluate. Add 150–170 μL TEV buffer to a final volume of 200 μL . Load this mixture on the prewashed centrifugal filter and spin for 3 min.
5. Measure the filtrate and estimate how much volume of liquid went through the filter. Add enough TEV buffer to the retentate to a final volume of 200 μL . Mix the sample by gently pipetting up and down without touching the membrane. Spin for 3 min.
6. Estimate the retained volume by checking the liquid on the filter or by measuring the volume of liquid that went through. Spin another 1 min or so until final volume is ~20–25 μL .
7. To collect the sample, place the filter inverted on a new collection tube. Spin at $1000 \times g$ for 3 min. Take an aliquot (10% of TEV-depleted sample volume) for SDS-PAGE analysis later (Subheading 3.6).

3.3.4 Buffer Exchange

The penultimate step prior to native MS analysis is buffer exchange, wherein the sample solution is switched into an electrospray-compatible solution of a volatile salt, typically ammonium acetate. We found that the most efficient buffer exchange method is by using Zeba microspin desalting columns (see **Note 11**). These spin columns contain 75 μL bed volume of gel filtration resin and are available with MWCO of 7 kDa (Zeba-7k) or 40 kDa (Zeba-40k) (see **Note 12**).

Significant sample loss has been observed from buffer exchanging samples into solutions with no passivating agent. We found that addition of a small amount of Tween-20 (0.001–0.01% v/v) in the buffer exchange solution enables maximum sample recovery without interference in subsequent MS analysis using the Exactive Plus EMR instrument [21].

All centrifuge spins are performed at 4 °C with either $1000 \times g$ (Zeba-7k) or $1500 \times g$ (Zeba-40k).

1. Flick or shake the spin column to remove bubbles and to ensure that the resin packs at the bottom.
2. Remove the column's bottom plug and loosen the top cap. Place the column in a 2-mL capless collection tube and centrifuge for 1 min to remove the storage solution.
3. Discard flowthrough. After each spin, the resin should appear white and free of liquid.
4. Place the column into the collection tube and add 50 μL of BE buffer. Spin for 1 min.
5. Discard flowthrough. Repeat the previous step three more times to fully wash and equilibrate the gel filtration resin with the BE solution.
6. Load 12–13 μL sample on top of the resin. Place on a clean 1.5 mL microfuge tube for sample collection. Spin for 2 min. Collect flowthrough and keep on ice.
7. Measure the collected volume. Take an aliquot (10% of the buffer-exchanged sample volume) for SDS-PAGE analysis (Subheading 3.6).
8. Proceed with native MS analysis of the buffer-exchanged samples (Subheading 3.5.2).

3.4 Preparation of Gold-Coated Emitters for Nanospray Native MS Analysis

Sample analysis by native MS is typically performed with an offline, static nanospray setup [35]. In this configuration, a small aliquot of the sample is loaded into a gold-coated glass or quartz emitter with a tip inner diameter (ID) of 1–5 μm to enable electrospray at nanoflow rates (10–50 nL/min). Sample introduction at low flow rates enables minimal sample consumption, efficient desolvation and reduced chemical background [35]. The conductive emitters are typically prepared in-house and are made in advance prior to native MS experiments.

3.4.1 Production of Emitters with a Laser Puller

The protocol presented here uses the Sutter Tip Puller Model P-2000. Always wear gloves when holding emitters to prevent contaminating the emitter surface, which can lead to uneven gold layer formation during sputter coating. The tips of the pulled emitters are delicate—handle them with care.

1. On the laser puller instrument, setup a program with the following parameters: Heat = 500, Fil = 0, Vel = 30, Del = 135, Pull = 175. These parameters can be adjusted depending on the desired tip shape of the emitters (see **Note 13**).
2. Load one capillary into the puller. Make sure it is centered relative to the laser. Clamp the capillary by tightening the knobs on both sides.
3. Close the lid and press the <PULL> button. A successful pulling cycle yields two emitters from one capillary.

4. Inspect each emitter to ensure that it is free of cracks and that the tip has the right shape (see tip shape in Fig. 1a) (see **Notes 14** and **15**).
5. Arrange the good-quality emitters on an inverted watch glass with two layers of double-sided tape placed on two opposing sides (about 2 cm away from the edge of each side). The sharp end of the emitter must be pointing towards the center. Each watch glass can accommodate a total of 50 emitters with 25 emitters at each side (Fig. 1b).

3.4.2 Sputter Coating of Emitters

The protocol outlined here uses an Edwards S150 Sputter Coater with a gold stage.

1. Turn the water chiller on 2 h before use. Set water temperature setting to 8 °C.
2. Turn the argon gas valve on (~3 psi).
3. To load the emitters, open the top lid of the sputter coater and remove the cylindrical covers. Carefully place the inverted watch glass containing the pulled emitters at the middle of the central platform. Replace the covers and the lid.
4. Turn on the mechanical rotary pump. After 5 min, turn on the Pirani gauge switch.
5. Flush the system with argon gas three times. In-between flushing steps, wait until the vacuum becomes stable with pressure ~1-10 mTorr. The pump down to reach this pressure takes about 5 min.
6. To initiate the coating, set the high voltage by pressing the HT button. Adjust the HT knob setting to 7. Turn the argon gas valve setting to 30-40. Adjust argon gas flow until the current reaches ~8 mA. A plasma discharge should be seen inside the chamber. Sputter coat for 1.5 min.
7. Turn off the voltage by turning the HT knob to zero. Reduce argon gas entry to zero. Wait until the pressure stabilizes.
8. Perform 3-4 more rounds of sputter coating by repeating **steps 6** and **7**.
9. When finished with sputter-coating, turn the Pirani gauge off. Then turn the rotary pump off. Vent the chamber by slowly opening the "air admit" valve. Remove the gold-coated emitters.
10. Repeat **steps 3-9** for the next batch of emitters.
11. Using plastic tweezers, carefully transfer the gold-coated emitters into a petri dish with double-sided tape or in a box of emitter holders for storage (see **Note 16**).

3.5 Native MS Analysis

We use the Exactive Plus EMR, an Orbitrap-based instrument configured for transmission and mass measurement of macromolecular assemblies at high resolving power (Fig. 2) [28] (see **Note 17**). The Nanoflex Ion Source for the EMR has a protective mounting that houses the emitter holder and nanospray source head. We removed this plastic housing to enable easy access to the emitter tip during MS analysis. In this protocol, the tip opening step involves a very light brushing motion with a gel-loading tip that immediately initiates electrospray with the high voltage turned on (Fig. 1c) (see **Note 18**). Making the source head and emitter tip accessible also enables facile reopening of the tip when there is suspected buildup or clogging.

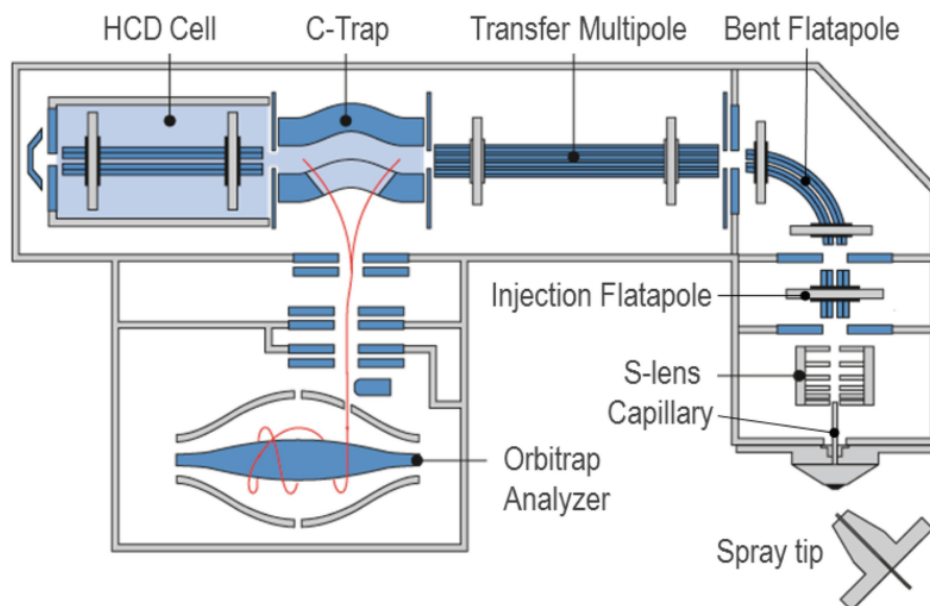


Fig. 2

Instrument schematic of the Exactive Plus EMR mass spectrometer. As the sample is being electrosprayed into the vacuum of the source region, the generated ions transit through the heated capillary and several ion transmission and focusing modules including the stacked ring ion guide (S-lens), injection flatapole, bent flatapole, and transport octapole. The voltage offsets in these modules can be manually tuned to enable mass filtering of the incoming protein ions. The bent flatapole also removes neutral particles (e.g., solvent droplets, neutral gas) as these cannot follow the ion trajectory dictated by the flatapole's geometry. The voltage difference between the injection and bent flatapoles is set as the interflatapole voltage. For efficient trapping and desolvation, the protein ions are stored in the higher-energy collisionally induced dissociation (HCD) cell that contains nitrogen gas for collisional cooling. After reaching a certain target ion population (automatic gain control or AGC) or a set injection time, the ions are transferred to the C-trap and then pulsed into the Orbitrap analyzer for mass measurement. In-source dissociation (ISD) and HCD CE can be adjusted by varying the voltage offset between the S-lens and the injection flatapole or the C-Trap and gas-containing HCD cell, respectively (Reproduced with permission from Thermo Fisher Scientific)

Caution must be taken not to directly touch the emitter tip or the source region when the high voltage is on. Avoid touching the hot inlet region where the heated capillary is located.

3.5.1 Instrument Calibration

We use aqueous cesium iodide solution with multiple CsI clusters $[(\text{CsI})_n\text{Cs}]^+$ as calibrant with a predefined calibration setting for the EMR encompassing 392.7–11,304.7 Th. Calibration is typically performed every 3–4 weeks.

1. Prepare an aqueous solution of 20 $\mu\text{g}/\mu\text{L}$ cesium iodide.
2. Operate the instrument as described in Subheading 3.5.2, **steps 1–10** with the calibrant solution as the sample.
3. For calibration, typical MS parameters include capillary temperature, 150 °C; spray voltage, 0.9–1.0 kV; ISD, 25–35 V; HCD CE, 100–125 V; S-lens RF level, 200; resolving power, 70,000 at m/z of 200; AGC target, 1×10^6 , number of microscans, 3; maximum injection time, 200 ms; injection flatapole, 4–8 V; interflatapole, 4 V; bent flatapole, 4 V; ultrahigh vacuum pressure, $6\text{--}8 \times 10^{-10}$ mbar.
4. Ensure that the spray is stable and that peaks up to 12,000 m/z have good intensities.
5. Perform eFT calibration and mass calibration on the positive EMR mode. The accuracy for the masses of CsI clusters postcalibration is typically below 2 ppm.
6. Since the calibrant is a nonvolatile salt solution, perform the calibration as quickly as possible to minimize salt accumulation at the source. To clean the heated ion transfer capillary, turn the EMR mode off and remove the capillary from the source. Rinse the inside of the transfer capillary with three rounds of water (~100 mL each) and then with 50 mL of 100% methanol before putting it back into the source.

3.5.2 Native MS Analysis of Endogenous Exosome Assemblies

1. With a ceramic glass cutter, shorten the gold-coated emitter by trimming ~1.5 cm from its flat end. This allows the emitter to fit into the sample holder in the source assembly and makes sample loading easier.
2. Using a gel-loading tip, load 2–3 μL of the buffer-exchanged sample into the emitter by carefully inserting the pipette tip as far into the emitter as possible and then slowly depositing the sample.
3. To fully push the sample into the emitter tip and to remove air bubbles, mount the emitter into the spin adapter assembly (Fig. 1a). Load into a small tabletop centrifuge and spin briefly (~10 s).
4. Pull the nanospray stage to extend and disengage it from the source. Using tweezers, gently insert the emitter starting with the flat end side into the static nanospray source head leaving about 5–8 mm of the emitter's sharp end protruding. Tighten the fitting to finger-tight (see **Note 19**).
5. Set the handheld vacuum pump to positive pressure and press to generate a small pressure on the emitter (gauge dial just moves slightly above zero). If the pressure dial starts decreasing, check for leaks and repressurize (see **Note 20**).
6. Push the nanospray stage to lock into the source and establish the high voltage connection. Move the emitter assembly closer to the source (3–10 mm from the ion transfer tube orifice) using the knobs that adjust the XYZ stage.
7. Load a tune file for native MS analysis. For the exosome complex, typical MS parameters include spray voltage, 0.9–1.2 kV; capillary temperature, 150 °C; S-lens RF level, 200; resolving power, 17,500 at m/z of 200; AGC target, 1×10^6 , number of microscans, 5; maximum injection time, 200 ms; injection flatapole, 8 V; interflatapole, 4 V; bent flatapole, 4 V; ultrahigh vacuum pressure, $6\text{--}8 \times 10^{-10}$ mbar.
8. Turn the capillary voltage on. The typical voltage setting is 0.9–1.2 kV.
9. Gently break open the emitter tip by lightly brushing it with a gel-loading tip (Fig. 1c) (see **Note 18**). Wait for a few seconds for peak signals to appear.
10. Once the electrospray is initiated and peaks consistently appear on the spectrum, optimize the signal and spray stability by adjusting the emitter distance and the spray voltage (see **Notes 21–23**).
11. Once a stable spray is established, adjust the front-end voltages to optimize ion transmission and detection of target species. Check the peak widths and aim for narrower peaks. Notably, the major limiting factor for achieving high mass resolution in native MS is the incomplete removal of adducts and solvent molecules (including water and ammonium acetate) that remain bound to the protein complex [36]. Efficient desolvation leads to higher sensitivity and resolution. To increase desolvation efficiency, adjust one or more of the following: heated capillary temperature, ISD voltage, HCD setting, and trapping gas pressure. It is important to be aware of the balance between increasing the energy for desolvation (narrower peaks for the intact complex) and gas-phase activation of the complex yielding dissociation (protein complex falls apart yielding additional peaks corresponding to subcomplexes).
12. Adjust the instrument resolution setting, if necessary. To resolve heterogeneities arising from posttranslational modifications, binding of small molecules (ligand or cofactor) and adduction, higher resolution is required. Note that higher resolution analysis involves longer analyzer transient times that yield lower peak intensities due to ion loss during detection (see **Note 24**).
13. Collision-induced dissociation can be achieved in-source (by increasing the ISD voltage) or within the HCD collision cell (by increasing the HCD CE parameter and the trapping gas pressure) (see **Note 25**). To systematically determine the optimal CID parameters, ramp the ISD or HCD CE voltages in increments of

- 10 V. Note the changes in the spectrum including the appearance of additional peak series across entire the m/z range.
14. Acquire at least 100 scans for each specific MS setting used. In addition, save the corresponding Tune File wherein MS parameters have been optimized.
 15. After sample analysis is finished, turn the high voltage off. Disengage the nanospray stage from the source. Depressurize the emitter by venting the handheld vacuum pump before removing emitter from the source head.
 16. After instrument use, set the EMR Mode to Off (trapping gas pressure setting of 1 and UHV pressure reaches $\sim 1.2 \times 10^{-10}$ mbar or lower). Set the capillary temperature to 250 °C. Put the EMR instrument on Standby mode.

3.5.3 Data Processing

Manual peak picking and deconvolution of the native MS spectrum described here can be performed for well-resolved peaks. For analyzing complicated spectra, the use of automated deconvolution software such as UniDec [37, 38] is advisable (see **Note 26**).

1. Open the Thermo RAW File using the Thermo Xcalibur Qual Browser.
2. Examine the spectrum for peak patterns. The peak series for each species typically exhibits a Gaussian-shaped charge-state distribution. The positive charges on the protein complex mainly comes from protonation of the basic sites on its surface. For two consecutive charge-state peaks with centroids at mass-to-charge ratios $(\frac{m}{z})$ and $(\frac{m}{z})_{z-1}$, where $(\frac{m}{z})_{z-1} = (m - m_{H^+}) / (z - 1)$ and the average mass of H^+ (m_{H^+}) is 1.007 Da, the charge-state z can be calculated using the formula:

$$z = \frac{(\frac{m}{z})_{z-1} - 1.007}{(\frac{m}{z})_{z-1} - (\frac{m}{z})}$$

3. With the calculated charge-states (each rounded off to the nearest whole number) for each peak in the peak series, compute the mass m for each charge-state species with $m = ((\frac{m}{z}) - 1.007) \times z$. One can setup the equations and perform the corresponding calculations in Microsoft Excel. Calculate the mean and standard deviation of all the mass m determined for each charge-state across the full charge-state distribution.
4. Table 1 lists the masses for the subunits of Exo-10 and associated proteins. Since Csl4, a constitutive component of the exosome core, was tagged for affinity capture, cytoplasmic- and nuclear-localized proteins that associate with the respective compartment-specific exosome core complexes were observed.

From the representative native MS spectrum on Fig. 3b, the main peak series that centers at 9500 Th corresponds to Exo-10 ($403,235 \pm 15$ Da). Furthermore, the identified subcomplexes and proteins include Exo-10 that lost Csl4p ($365,762 \pm 7$ Da), Mtr3p/Dis3p/Rrp4p/Rrp41p/Rrp42p/Rrp45p ($271,032 \pm 13$ Da),

Dis3p/Rrp4p/Rrp41p/Rrp42p/Rrp45p ($243,412 \pm 3$ Da), Ski complex composed of Ski8p/Ski2p/Ski3p at 2:1:1 stoichiometry ($398,229 \pm 9$ Da), Ski7p ($84,812 \pm 5$ Da), and Mtr4p ($122,089 \pm 2$ Da). From gas-phase dissociation, both the Exo-10 core and Exo-10 that lost Csl4p were activated and ejected Rrp40p yielding two charge-stripped subcomplexes with masses of $376,793 \pm 4$ Da and $339,310 \pm 12$ Da, respectively (see **Note 25**).

Table 1

Intact average masses of subunits comprising the affinity-isolated endogenous exosome complex and associated proteins from budding yeast

Protein	Sequence mass (Da)^a	Modifications^b	Expected mass (Da)^c
<i>Core components</i>			
Csl4p-TAP	52,631.6	-Met, N-term Ac, TEV protease cleavage	37,460.0
Dis3p	113,706.6	-Met, N-term Ac	113,617.5
Rrp4p	39,427.2	-Met, N-term Ac	39,338.1
Rrp43p	44,011.0	-Met, N-term Ac	43,921.9
Rrp45p	33,961.9	-Met, N-term Ac	33,872.7
Rrp42p	29,055.2	-Met, N-term Ac	28,966.0
Mtr3p	27,577.0	N-term Ac	27,619.0
Rrp41p	27,560.7	-Met, N-term Ac	27,471.5
Rrp46p	24,407.2	-Met, N-term Ac	24,318.1
Rrp40p	26,556.4	-Met, N-term Ac	26,467.2
Rrp6p	84,038.5	-Met, N-term Ac	83,949.3
<i>Nuclear-specific</i>			
Ski7p	84,778.8	-Met, N-term Ac	84,689.7
Lrp1p	21,087.2		21,087.2
<i>Cytoplasmic-specific</i>			
Ski2p	146,058.4	-Met, N-term Ac	145,969.2
Ski8p	44,231.6		44,231.6
Ski3p	163,725.8		163,725.8
Mtr4p	122,054.9	N-term Ac	122,096.9

Table reproduced with permission from ref. 21. Copyright 2016 American Chemical Society

^aMass from the primary sequence of the full-length and unprocessed protein

^bThis includes protease cleavage during native elution and also N-terminal processing or co-translational modifications, such as N-terminal methionine removal and acetylation obtained from bottom-up LC-MS analysis, native MS analysis, and publicly available proteomic databases: Saccharomyces Gene Database (SGD), Global Proteome Machine (GPM) and Uniprot. Additional mass information was obtained from refs. [17](#), [18](#), [21](#)

^cMass of the mature protein obtained after accounting for processing and modifications

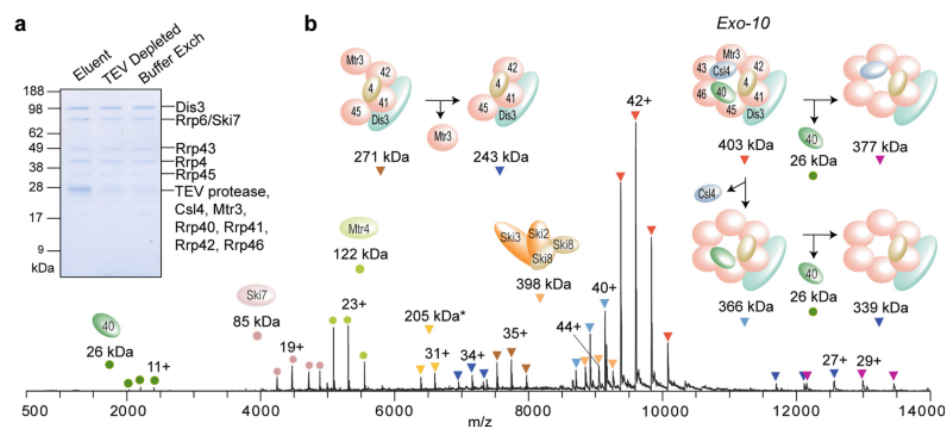


Fig. 3

Native MS analysis of the affinity-captured endogenous exosome assembly from budding yeast. **(a)** SDS-PAGE analysis of aliquots (10% of each sample) from each postelution step in the workflow showed minimal losses at each sample handling step. **(b)** Representative native MS spectrum of the exosome complex with corresponding peak and mass assignments. A model of the Exo-10 core assembly is presented to show subunit arrangement based on previous studies [[17](#), [18](#), [50](#)]. The charge-state for the most intense peak within each charge-state distribution is indicated (Reproduced with permission from ref. [21](#). Copyright 2016 American Chemical Society)

3.6 SDS-PAGE Analysis to Assess Sample Handling Steps

1. After the eluted sample has been collected, add 20 μ L of 1% SDS solution or SDS-PAGE gel loading buffer with no DTT to the magnetic beads. Incubate at RT for 15 min.
2. Place in magnet and collect the bead-retained sample. Measure the volume and take an aliquot (10% of the bead-bound residual sample) for SDS-PAGE analysis.

3. Perform SDS-PAGE analysis of the collected aliquots (TEV eluate, TEV-depleted, buffer-exchanged, and bead-bound residual) to check for sample loss during each step of sample handling (Fig. 3a).

4 Notes

1. Another native MS analyzer that is commonly used is a quadrupole time-of-flight (Q-ToF); it has tandem MS capability enabling specific mass selection and subsequent gas-phase activation of protein complexes [39, 40]. The Synapt (Waters) is a commercially available Q-ToF instrument with an integrated ion mobility module [41]. Protocols for performing native MS analysis using the Synapt instrument can be found in [42, 43].
2. The Exactive EMR off-line kit comes with the syringe-and-backing plate setup that provides backpressure during electrospray. However, this setup has no pressure readout and can be cumbersome to operate. In our hands, the handheld vacuum pump is easier to use as it only requires gripping the handle to generate pressure. It also has a pressure gauge and enables detection of pressure leaks. The handheld pump can be purchased from online stores such as Amazon.
3. In some cases, the rattling sound disappears after a few milling cycles. One possible reason is that the cell powder has caked inside the jar. If caking is suspected, open the jar assembly, remove all the balls and scrape the inner walls of the jar with a prechilled spatula to dislodge the caked material prior to proceeding with the next milling cycle.
4. Ensure that the IgG stock solution does not contain glycerol or buffer components (when the IgG sample was prepared immediately prior to lyophilization) with amine, hydroxyl, or sulfhydryl moieties that can quench the reactive epoxy groups on the magnetic beads. If these reagents are present, buffer exchange the IgG stock into 0.1 M sodium phosphate, pH 7.4 or PBS prior to conjugation.
5. Initially keeping the AC buffer at room temperature facilitates quick resuspension of the frozen cell powder.
6. This corresponds to 4 mg of IgG-conjugated magnetic beads (40 μ L \times 0.1 mg/ μ L beads) for 0.5 g of cryomilled cell powder (~250 mL of yeast cell culture). This bead:cell powder proportion is typically sufficient for efficient capture (> 70%) of the tagged exosome complex.
7. Incubation times of 30–60 min is sufficient to capture the target protein complexes with minimal accumulation of nonspecific proteins [25].
8. A competitive elution peptide, PEGyIOx has been developed that releases protein A-tagged (including TAP-tagged) complexes from IgG-conjugated beads [30]. After elution, the peptide, which is typically used at ~2 mM concentration, can be effectively depleted by buffer exchanging into a Zeba-40k spin column.
9. The on-bead protease elution step is most effective when performed in small volumes (10–20 μ L) with protease concentrations of ~1–5 μ M (25–125 ng/ μ L).
10. Alternative methods to deplete the protease include (a) another round of affinity isolation step for the target protein complex (for TAP tags, this involves affinity capture with calmodulin-coated beads and subsequent EGTA elution)[17, 18, 19, 20], (b) metal affinity chromatography (removal via the polyhistidine tag on the ActEV protease), or (c) size exclusion chromatography. However, these methods require longer sample processing times which can lead to the dissociation of less stable protein complexes and sample loss.
11. Alternative methods for buffer exchange include gel filtration, centrifugation with a filter membrane, or dialysis. These techniques involve longer sample handling times. Moreover, ~12 μ L of buffer-exchanged sample from the microspin desalting columns is sufficient for native MS analysis as only a few μ L of sample is loaded in emitters and sprayed at nanoflow rates.
12. According to the manufacturer's guide (Thermo Fisher Scientific), the Zeba-7k effectively traps and retains buffer components with mass <0.8 kDa whereas the Zeba-40k removes components with mass <1.5 kDa. After buffer exchange on a Zeba-7k, no additional volume apart from the initial volume loaded is recovered. In contrast, some sample dilution is observed with Zeba-40k (addition of ~2–4 μ L to the initial volume).
13. The parameters for laser pulling are typically determined empirically and are puller-dependent. According to the manufacturer's instructions (Sutter), the parameter Heat sets the amount of laser energy supplied to the capillary, Vel (Velocity) relates to the glass temperature and determines the trip point for the hard pull, Del (Delay) sets the time (in ms) when the hard pull gets activated after the laser heating turns off, and Pull controls the force of the hard pull. The main parameters that usually get optimized include Heat, which varies depending on the age and power of the laser, and Delay, with shorter times yielding emitters with smaller inner diameter.
14. Inspection by eye is usually sufficient to spot broken emitters or emitters with irregular shape. One can also use a simple microscope for inspection of a few emitters to have a better sense of tip structure.

15. If the two emitters that formed from one capillary differ in shape and taper dimensions, check for the vertical alignment of the laser. With gloves on, remove the shroud that covers the gold retro mirror using a screw driver. Load a capillary tip. Place a piece of thermal fax paper in-between the capillary and the concave gold retro mirror. The shiny part of the fax paper must face the capillary. Close the lid. Input these parameters: Heat = 200, Fil = 5, Delay = 40. Press <PULL>. After the pull cycle, check the fax paper. For a well-aligned laser, two thick, symmetric lines (dark ellipses) are observed. If either line is thicker than the other, adjust the micrometer at the back of the instrument. Repeat the cycle until the two lines are symmetric.
16. It is recommended to remove the coated emitters at the area above the double-sided tape where there is less gold coating and is far enough from the emitter's sharp end. The adhesive tape should be less sticky after the sputter coating process.
17. The first-generation Exactive Plus EMR instrument used here can only perform all-ion fragmentation (AIF) wherein all the incoming ions are activated but no specific mass selection is achieved for subsequent tandem MS [28]. The next generation of Exactive EMR instruments have additional modifications including replacement of the transport multipole with a quadrupole analyzer for tandem or multistage fragmentation. This allows for selection of protein complexes within a certain m/z range for gas-phase dissociation and subsequent isolation of an ejected subunit for further fragmentation [44, 45, 46].
18. The two alternative ways of opening the emitter tip include (a) trimming it with tweezers under a microscope before loading onto the source or (b) placing the emitter on the source stage and touching the emitter tip against the wall close to the orifice of the heated ion transfer tube. Both methods involve extra time. Moreover, the second method requires maneuvering of the source camera while positioning the tip and that the tip breaking be performed as quickly as possible because of direct contact with the hot source interface.
19. Overtightening the fitting can shorten the lifetime of the electrically conducting rubber ferrule that contacts the emitter inside the nanospray source head.
20. Alternatively, if using the gas-tight syringe with a black plate (comes with the nanospray kit) to generate backpressure, press the plunger to about a quarter or halfway through and lock into place by mounting the syringe into a slot of the black plate.
21. If the spray is unstable, the sample might be aggregating and crashing out of solution. Increase the backpressure to the sample. If this does not work, reopen the emitter. To further address sample aggregation, dilute the sample or optimize ammonium acetate solution conditions (e.g., pH and ionic strength).
22. Instabilities in the spray might also arise from a problematic emitter either from loss of conductive coating or aberrant tip shape. Replace the emitter. Transfer the sample that is deposited in the problematic emitter into a new emitter or load a fresh aliquot of sample.
23. If no electrospray occurs (droplets forming at the tip), check the high voltage contact between the emitter and the source. Inspect the gold coating on the emitter. Check the conductive ferrule in the source head; replace if worn out and damaged.
24. Orbitrap MS detection involves recording of the image current transients from the axial oscillations of the ions in the analyzer; longer transient times result in mass measurements of higher resolution [47]. However, during the detection process, the ions can collide with residual gas in the analyzer causing potential diffusion, incoherence, dissociation, and fragmentation, leading to substantial ion loss [48]. This loss can be particularly worse with macromolecular assemblies having large collision cross-sections leading to a significant decrease in peak intensity at higher resolution settings.
25. Gas phase dissociation of protein complexes by collision induced dissociation (CID) involves activation of the protein complex by collisions with gas molecules as the ions accelerate into a chamber. The internal energy from the collisional "heating" gets dissipated mainly through unfolding of a subunit that eventually gets ejected taking with it a disproportionately large fraction of the charge from the parent complex and leaving a lower charge-density ("charge-stripping") on the corresponding subcomplex [49].
26. The UniDec software is freely available and can be downloaded from the Marty Lab website at <https://marty.lab.arizona.edu/content/software>. The website has a tutorial and a link to the software source code.

Notes

Acknowledgments

This work is supported by National Institutes of Health grants P41 GM103314 and P41 GM109824. We gratefully acknowledge the members of the Chait lab and the Laboratory of Cellular and Structural Biology (headed by Professor Michael Rout) at the Rockefeller University for feedback and insightful discussions. We especially thank Andrew Krutchinsky for the design and implementation of the modifications in the nanoelectrospray setup described here. We also thank Zhanna Hakhverdyan for providing the cryomilled yeast powder.

References

1. Hartwell L, Hopfield J, Leibler S, Murray A (1999) From molecular to modular cell biology. *Nature* 402:C47–C52
PubMed (http://www.ncbi.nlm.nih.gov/entrez/query.fcgi?cmd=Retrieve&db=PubMed&dopt=Abstract&list_uids=10591225)
Google Scholar (http://scholar.google.com/scholar_lookup?title=From%20molecular%20to%20modular%20cell%20biology&author=L.%20Hartwell&author=J.%20Hopfield&author=S.%20Leibler&author=A.%20Murray&journal=Nature&volume=402&pages=C47-C52&publication_year=1999)
2. Robinson CV, Sali A, Baumeister W (2007) The molecular sociology of the cell. *Nature* 450:973–982
PubMed (http://www.ncbi.nlm.nih.gov/entrez/query.fcgi?cmd=Retrieve&db=PubMed&dopt=Abstract&list_uids=18075576)
Google Scholar (http://scholar.google.com/scholar_lookup?title=The%20molecular%20sociology%20of%20the%20cell&author=CV.%20Robinson&author=A.%20Sali&author=W.%20Baumeister&journal=Nature&volume=450&pages=973-982&publication_year=2007)
3. Alber F, Förster F, Korkin D et al (2008) Integrating diverse data for structure determination of macromolecular assemblies. *Annu Rev Biochem* 77:443–477
PubMed (http://www.ncbi.nlm.nih.gov/entrez/query.fcgi?cmd=Retrieve&db=PubMed&dopt=Abstract&list_uids=18318657)
Google Scholar (http://scholar.google.com/scholar_lookup?title=Integrating%20diverse%20data%20for%20structure%20determination%20of%20macromolecular%20assemblies&author=F.%20Alber&author=F.%20F%C3%B6rster&author=D.%20Korkin&journal=Annu%20Rev%20Biochem&volume=77&pages=443-477&publication_year=2008)
4. Lössl P, van de Waterbeemd M, Heck AJ et al (2016) The diverse and expanding role of mass spectrometry in structural and molecular biology. *EMBO J* 16:155–166
Google Scholar (http://scholar.google.com/scholar_lookup?title=The%20diverse%20and%20expanding%20role%20of%20mass%20spectrometry%20in%20structural%20and%20molecular%20biology&author=P.%20L%C3%B6ssl&author=M.%20Waterbeemd&author=AJ.%20Heck&journal=EMBO%20J&volume=16&pages=155-166&publication_year=2016)
5. Chait BT, Cadene M, Olinares PD et al (2016) Revealing higher order protein structure using mass spectrometry. *J Am Soc Mass Spectrom* 27:952–965
PubMed (http://www.ncbi.nlm.nih.gov/entrez/query.fcgi?cmd=Retrieve&db=PubMed&dopt=Abstract&list_uids=27080007)
PubMedCentral (<http://www.ncbi.nlm.nih.gov/pmc/articles/PMC5125627>)
Google Scholar (http://scholar.google.com/scholar_lookup?title=Revealing%20higher%20order%20protein%20structure%20using%20mass%20spectrometry&author=BT.%20Chait&author=M.%20Cadene&author=PD.%20Olinares&journal=J%20Am%20Soc%20Mass%20Spectrom&volume=27&pages=952-965&publication_year=2016)
6. Loo J (1997) Studying noncovalent protein complexes by electrospray ionization mass spectrometry. *Mass Spectrom Rev* 16:1–23
PubMed (http://www.ncbi.nlm.nih.gov/entrez/query.fcgi?cmd=Retrieve&db=PubMed&dopt=Abstract&list_uids=9414489)
Google Scholar (http://scholar.google.com/scholar_lookup?title=Studying%20noncovalent%20protein%20complexes%20by%20electrospray%20ionization%20mass%20spectrometry&author=J.%20Loo&journal=Mass%20Spectrom%20Rev&volume=16&pages=1-23&publication_year=1997)
7. Heck AJR (2008) Native mass spectrometry: a bridge between interactomics and structural biology. *Nat Methods* 5:927–933
PubMed (http://www.ncbi.nlm.nih.gov/entrez/query.fcgi?cmd=Retrieve&db=PubMed&dopt=Abstract&list_uids=18974734)
Google Scholar (http://scholar.google.com/scholar_lookup?title=Native%20mass%20spectrometry%3A%20a%20bridge%20between%20interactomics%20and%20structural%20biology&author=AJR.%20Heck&journal=Nat%20Methods&volume=5&pages=927-933&publication_year=2008)
8. Taverner T, Hernández H, Sharon M et al (2008) Subunit architecture of intact protein complexes from mass spectrometry and homology modeling. *Acc Chem Res* 41:617–627
PubMed (http://www.ncbi.nlm.nih.gov/entrez/query.fcgi?cmd=Retrieve&db=PubMed&dopt=Abstract&list_uids=18314965)
Google Scholar (http://scholar.google.com/scholar_lookup?title=Subunit%20architecture%20of%20intact%20protein%20complexes%20from%20mass%20spectrometry%20and%20homology%20modeling&author=T.%20Taverner&author=H.%20Hern%C3%A1ndez&author=M.%20Sharon&journal=Acc%20Chem%20Res&volume=41&pages=617-627&publication_year=2008)
9. Leney AC, Heck AJR (2017) Native mass spectrometry: what is in the name? *J Am Soc Mass Spectrom* 28:5–13
PubMed (http://www.ncbi.nlm.nih.gov/entrez/query.fcgi?cmd=Retrieve&db=PubMed&dopt=Abstract&list_uids=32020797)
Google Scholar (http://scholar.google.com/scholar_lookup?title=Native%20mass%20spectrometry%3A%20what%20is%20in%20the%20name%3F&author=AC.%20Leney&author=AJR.%20Heck&journal=J%20Am%20Soc%20Mass%20Spectrom&volume=28&pages=5-13&publication_year=2017)

10. Snijder J, Heck AJR (2014) Analytical approaches for size and mass analysis of large protein assemblies. *Annu Rev Anal Chem (Palo Alto, Calif)* 7:43–64
[Google Scholar](#) (http://scholar.google.com/scholar_lookup?title=Analytical%20approaches%20for%20size%20and%20mass%20analysis%20of%20large%20protein%20assemblies&author=J.%20Snijder&author=A.JR.%20Heck&journal=Annu%20Rev%20Anal%20Chem%20%28Palo%20Alto%2C%20Calif%29&volume=7&pages=43-64&publication_year=2014)
11. Marcoux J, Robinson CV (2013) Twenty years of gas phase structural biology. *Structure* 21:1541–1550
[PubMed](#) (http://www.ncbi.nlm.nih.gov/entrez/query.fcgi?cmd=Retrieve&db=PubMed&dopt=Abstract&list_uids=240101713)
[Google Scholar](#) (http://scholar.google.com/scholar_lookup?title=Twenty%20years%20of%20gas%20phase%20structural%20biology&author=J.%20Marcoux&author=CV.%20Robinson&journal=Structure&volume=21&pages=1541-1550&publication_year=2013)
12. Erba EB, Petosa C (2015) The emerging role of native mass spectrometry in characterizing the structure and dynamics of macromolecular complexes. *Protein Sci* 24:1176–1192
[Google Scholar](#) (http://scholar.google.com/scholar_lookup?title=The%20emerging%20role%20of%20native%20mass%20spectrometry%20in%20characterizing%20the%20structure%20and%20dynamics%20of%20macromolecular%20complexes&author=EB.%20Erba&author=C.%20Petosa&journal=Protein%20Sci&volume=24&pages=1176-1192&publication_year=2015)
13. Gavin A-C, Aloy P, Grandi P et al (2006) Proteome survey reveals modularity of the yeast cell machinery. *Nature* 440:631–636
[PubMed](#) (http://www.ncbi.nlm.nih.gov/entrez/query.fcgi?cmd=Retrieve&db=PubMed&dopt=Abstract&list_uids=16429126)
[Google Scholar](#) (http://scholar.google.com/scholar_lookup?title=Proteome%20survey%20reveals%20modularity%20of%20the%20yeast%20cell%20machinery&author=A-C.%20Gavin&author=P.%20Aloy&author=P.%20Grandi&journal=Nature&volume=440&pages=631-636&publication_year=2006)
14. Krogan NJ, Cagney G, Yu H et al (2006) Global landscape of protein complexes in the yeast *Saccharomyces cerevisiae*. *Nature* 440:637–643
[PubMed](#) (http://www.ncbi.nlm.nih.gov/entrez/query.fcgi?cmd=Retrieve&db=PubMed&dopt=Abstract&list_uids=16554755)
[Google Scholar](#) (http://scholar.google.com/scholar_lookup?title=Global%20landscape%20of%20protein%20complexes%20in%20the%20yeast%20Saccharomyces%20cerevisiae&author=NJ.%20Krogan&author=G.%20Cagney&author=H.%20Yu&journal=Nature&volume=440&pages=637-643&publication_year=2006)
15. Mitchell P, Petfalski E, Shevchenko A et al (1997) The exosome: a conserved eukaryotic RNA processing complex containing multiple 3'→5' Exoribonucleases. *Cell* 91:457–466
[PubMed](#) (http://www.ncbi.nlm.nih.gov/entrez/query.fcgi?cmd=Retrieve&db=PubMed&dopt=Abstract&list_uids=9390555)
[Google Scholar](#) (http://scholar.google.com/scholar_lookup?title=The%20exosome%3A%20a%20conserved%20eukaryotic%20RNA%20processing%20complex%20containing%20multiple%203%E2%80%B2%E2%86%92%E2%80%B2%20Exoribonucleases&author=P.%20Mitchell&author=E.%20Petfalski&author=A.%20Shevchenko&journal=Cell&volume=91&pages=457-466&publication_year=1997)
16. Liu Q, Greimann JC, Lima CD (2006) Reconstitution, activities, and structure of the eukaryotic RNA exosome. *Cell* 127:1223–1237
[PubMed](#) (http://www.ncbi.nlm.nih.gov/entrez/query.fcgi?cmd=Retrieve&db=PubMed&dopt=Abstract&list_uids=17174896)
[Google Scholar](#) (http://scholar.google.com/scholar_lookup?title=Reconstitution%2C%20activities%2C%20and%20structure%20of%20the%20eukaryotic%20RNA%20exosome&author=Q.%20Liu&author=JC.%20Greimann&author=CD.%20Lima&journal=Cell&volume=127&pages=1223-1237&publication_year=2006)
17. Hernández H, Dziembowski A, Taverner T et al (2006) Subunit architecture of multimeric complexes isolated directly from cells. *EMBO Rep* 7:605–610
[PubMed](#) (http://www.ncbi.nlm.nih.gov/entrez/query.fcgi?cmd=Retrieve&db=PubMed&dopt=Abstract&list_uids=16729021)
[PubMedCentral](#) (<http://www.ncbi.nlm.nih.gov/pmc/articles/PMC1479597>)
[Google Scholar](#) (http://scholar.google.com/scholar_lookup?title=Subunit%20architecture%20of%20multimeric%20complexes%20isolated%20directly%20from%20cells&author=H.%20Hern%C3%A1ndez&author=A.%20Dziembowski&author=T.%20Taverner&journal=EMBO%20Rep&volume=7&pages=605-610&publication_year=2006)
18. Synowsky SA, van den Heuvel RHH, Mohammed S et al (2006) Probing genuine strong interactions and post-translational modifications in the heterogeneous yeast exosome protein complex. *Mol Cell Proteomics* 5:1581–1592
[PubMed](#) (http://www.ncbi.nlm.nih.gov/entrez/query.fcgi?cmd=Retrieve&db=PubMed&dopt=Abstract&list_uids=16829593)
[Google Scholar](#) (http://scholar.google.com/scholar_lookup?title=Probing%20genuine%20strong%20interactions%20and%20post-translational%20modifications%20in%20the%20heterogeneous%20yeast%20exosome%20protein%20complex&author=SA.%20Synowsky&author=RHH.%20Heuvel&author=S.%20Mohammed&journal=Mol%20Cell%20Proteomics&volume=5&pages=1581-1592&publication_year=2006)
19. Synowsky SA, Heck AJ (2008) The yeast ski complex is a hetero-tetramer. *Protein Sci* 17:119–125
[PubMed](#) (<http://www.ncbi.nlm.nih.gov/entrez/query.fcgi?>)

- cmd=Retrieve&db=PubMed&dopt=Abstract&list_uids=18042677)
[PubMedCentral](http://www.ncbi.nlm.nih.gov/pmc/articles/PMC2144600) (http://www.ncbi.nlm.nih.gov/pmc/articles/PMC2144600)
[Google Scholar](http://scholar.google.com/scholar_lookup?title=The%20yeast%20oski%20complex%20is%20a%20hetero-tetramer&author=SA.%20Synowsky&author=AJ.%20Heck&journal=Protein%20Sci&volume=17&pages=119-125&publication_year=2008) (http://scholar.google.com/scholar_lookup?title=The%20yeast%20oski%20complex%20is%20a%20hetero-tetramer&author=SA.%20Synowsky&author=AJ.%20Heck&journal=Protein%20Sci&volume=17&pages=119-125&publication_year=2008)
20. Synowsky SA, van Wijk M, Rajmakers R, Heck AJR (2009) Comparative multiplexed mass spectrometric analyses of endogenously expressed yeast nuclear and cytoplasmic exosomes. *J Mol Biol* 385:1300–1313
[PubMed](http://www.ncbi.nlm.nih.gov/entrez/query.fcgi?cmd=Retrieve&db=PubMed&dopt=Abstract&list_uids=19046973) (http://www.ncbi.nlm.nih.gov/entrez/query.fcgi?cmd=Retrieve&db=PubMed&dopt=Abstract&list_uids=19046973)
[Google Scholar](http://scholar.google.com/scholar_lookup?title=Comparative%20multiplexed%20mass%20spectrometric%20analyses%20of%20endogenously%20expressed%20yeast%20nuclear%20and%20cytoplasmic%20exosomes&author=SA.%20Synowsky&author=M.%20Wijk&author=R.%20Rajmakers&author=AJR.%20Heck&journal=J%20Mol%20Biol&volume=385&pages=1300-1313&publication_year=2009) (http://scholar.google.com/scholar_lookup?title=Comparative%20multiplexed%20mass%20spectrometric%20analyses%20of%20endogenously%20expressed%20yeast%20nuclear%20and%20cytoplasmic%20exosomes&author=SA.%20Synowsky&author=M.%20Wijk&author=R.%20Rajmakers&author=AJR.%20Heck&journal=J%20Mol%20Biol&volume=385&pages=1300-1313&publication_year=2009)
21. Olinares PDB, Dunn AD, Padovan JC et al (2016) A robust workflow for native mass spectrometric analysis of affinity-isolated endogenous protein assemblies. *Anal Chem* 88:2799–2807
[PubMed](http://www.ncbi.nlm.nih.gov/entrez/query.fcgi?cmd=Retrieve&db=PubMed&dopt=Abstract&list_uids=26849307) (http://www.ncbi.nlm.nih.gov/entrez/query.fcgi?cmd=Retrieve&db=PubMed&dopt=Abstract&list_uids=26849307)
[PubMedCentral](http://www.ncbi.nlm.nih.gov/pmc/articles/PMC4790104) (http://www.ncbi.nlm.nih.gov/pmc/articles/PMC4790104)
[Google Scholar](http://scholar.google.com/scholar_lookup?title=A%20robust%20workflow%20for%20native%20mass%20spectrometric%20analysis%20of%20affinity-isolated%20endogenous%20protein%20assemblies&author=PDB.%20Olinares&author=AD.%20Dunn&author=JC.%20Padovan&journal=Anal%20Chem&volume=88&pages=2799-2807&publication_year=2016) (http://scholar.google.com/scholar_lookup?title=A%20robust%20workflow%20for%20native%20mass%20spectrometric%20analysis%20of%20affinity-isolated%20endogenous%20protein%20assemblies&author=PDB.%20Olinares&author=AD.%20Dunn&author=JC.%20Padovan&journal=Anal%20Chem&volume=88&pages=2799-2807&publication_year=2016)
22. Rigaut G, Shevchenko A, Rutz B et al (1999) A generic protein purification method for protein complex characterization and proteome exploration. *Nat Biotechnol* 17:1030–1032
[PubMed](http://www.ncbi.nlm.nih.gov/entrez/query.fcgi?cmd=Retrieve&db=PubMed&dopt=Abstract&list_uids=10504710) (http://www.ncbi.nlm.nih.gov/entrez/query.fcgi?cmd=Retrieve&db=PubMed&dopt=Abstract&list_uids=10504710)
[Google Scholar](http://scholar.google.com/scholar_lookup?title=A%20generic%20protein%20purification%20method%20for%20protein%20complex%20characterization%20and%20proteome%20exploration&author=G.%20Rigaut&author=A.%20Shevchenko&author=B.%20Rutz&journal=Nat%20Biotechnol&volume=17&pages=1030-1032&publication_year=1999) (http://scholar.google.com/scholar_lookup?title=A%20generic%20protein%20purification%20method%20for%20protein%20complex%20characterization%20and%20proteome%20exploration&author=G.%20Rigaut&author=A.%20Shevchenko&author=B.%20Rutz&journal=Nat%20Biotechnol&volume=17&pages=1030-1032&publication_year=1999)
23. Puig O, Caspary F, Rigaut G et al (2001) The tandem affinity purification (TAP) method: a general procedure of protein complex purification. *Methods* 24:218–229
[PubMed](http://www.ncbi.nlm.nih.gov/entrez/query.fcgi?cmd=Retrieve&db=PubMed&dopt=Abstract&list_uids=11403571) (http://www.ncbi.nlm.nih.gov/entrez/query.fcgi?cmd=Retrieve&db=PubMed&dopt=Abstract&list_uids=11403571)
[Google Scholar](http://scholar.google.com/scholar_lookup?title=The%20tandem%20affinity%20purification%20method%20of%20general%20procedure%20of%20protein%20complex%20purification&author=O.%20Puig&author=F.%20Caspary&author=G.%20Rigaut&journal=Methods&volume=24&pages=218-229&publication_year=2001) (http://scholar.google.com/scholar_lookup?title=The%20tandem%20affinity%20purification%20method%20of%20general%20procedure%20of%20protein%20complex%20purification&author=O.%20Puig&author=F.%20Caspary&author=G.%20Rigaut&journal=Methods&volume=24&pages=218-229&publication_year=2001)
24. Oeffinger M, Wei KE, Rogers R et al (2007) Comprehensive analysis of diverse ribonucleoprotein complexes. *Nat Methods* 4:951–956
[PubMed](http://www.ncbi.nlm.nih.gov/entrez/query.fcgi?cmd=Retrieve&db=PubMed&dopt=Abstract&list_uids=17922018) (http://www.ncbi.nlm.nih.gov/entrez/query.fcgi?cmd=Retrieve&db=PubMed&dopt=Abstract&list_uids=17922018)
[Google Scholar](http://scholar.google.com/scholar_lookup?title=Comprehensive%20analysis%20of%20diverse%20ribonucleoprotein%20complexes&author=M.%20Oeffinger&author=KE.%20Wei&author=R.%20Rogers&journal=Nat%20Methods&volume=4&pages=951-956&publication_year=2007) (http://scholar.google.com/scholar_lookup?title=Comprehensive%20analysis%20of%20diverse%20ribonucleoprotein%20complexes&author=M.%20Oeffinger&author=KE.%20Wei&author=R.%20Rogers&journal=Nat%20Methods&volume=4&pages=951-956&publication_year=2007)
25. Cristea IM, Williams R, Chait BT, Rout MP (2005) Fluorescent proteins as proteomic probes. *Mol Cell Proteomics* 4:1933–1941
[PubMed](http://www.ncbi.nlm.nih.gov/entrez/query.fcgi?cmd=Retrieve&db=PubMed&dopt=Abstract&list_uids=16155292) (http://www.ncbi.nlm.nih.gov/entrez/query.fcgi?cmd=Retrieve&db=PubMed&dopt=Abstract&list_uids=16155292)
[Google Scholar](http://scholar.google.com/scholar_lookup?title=Fluorescent%20proteins%20as%20proteomic%20probes&author=IM.%20Cristea&author=R.%20Williams&author=BT.%20Chait&author=MP.%20Rout&journal=Mol%20Cell%20Proteomics&volume=4&pages=1933-1941&publication_year=2005) (http://scholar.google.com/scholar_lookup?title=Fluorescent%20proteins%20as%20proteomic%20probes&author=IM.%20Cristea&author=R.%20Williams&author=BT.%20Chait&author=MP.%20Rout&journal=Mol%20Cell%20Proteomics&volume=4&pages=1933-1941&publication_year=2005)
26. LaCava J, Fernandez-Martinez J, Hakhverdyan Z, Rout MP (2016) Optimized affinity capture of yeast protein complexes. *Cold Spring Harb Protoc* 2016:615–619
[Google Scholar](http://scholar.google.com/scholar_lookup?title=Optimized%20affinity%20capture%20of%20yeast%20protein%20complexes&author=J.%20LaCava&author=J.%20Fernandez-Martinez&author=Z.%20Hakhverdyan&author=MP.%20Rout&journal=Cold%20Spring%20Harb%20Protoc&volume=2016&pages=615-619&publication_year=2016) (http://scholar.google.com/scholar_lookup?title=Optimized%20affinity%20capture%20of%20yeast%20protein%20complexes&author=J.%20LaCava&author=J.%20Fernandez-Martinez&author=Z.%20Hakhverdyan&author=MP.%20Rout&journal=Cold%20Spring%20Harb%20Protoc&volume=2016&pages=615-619&publication_year=2016)
27. Hakhverdyan Z, Domanski M, Hough LE et al (2015) Rapid, optimized interactomic screening. *Nat Methods* 12:553–560
[PubMed](http://www.ncbi.nlm.nih.gov/entrez/query.fcgi?cmd=Retrieve&db=PubMed&dopt=Abstract&list_uids=25938370) (http://www.ncbi.nlm.nih.gov/entrez/query.fcgi?cmd=Retrieve&db=PubMed&dopt=Abstract&list_uids=25938370)
[PubMedCentral](http://www.ncbi.nlm.nih.gov/pmc/articles/PMC4449307) (http://www.ncbi.nlm.nih.gov/pmc/articles/PMC4449307)
[Google Scholar](http://scholar.google.com/scholar_lookup?title=Rapid%20optimized%20interactomic%20screening&author=Z.%20Hakhverdyan&author=M.%20Domanski&author=LE.%20Hough&journal=Nat%20Methods&volume=12&pages=553-560&publication_year=2015) (http://scholar.google.com/scholar_lookup?title=Rapid%20optimized%20interactomic%20screening&author=Z.%20Hakhverdyan&author=M.%20Domanski&author=LE.%20Hough&journal=Nat%20Methods&volume=12&pages=553-560&publication_year=2015)

28. Rose RJ, Damoc E, Denisov E et al (2012) High-sensitivity Orbitrap mass analysis of intact macromolecular assemblies. *Nat Methods* 9:1084–1086
PubMed (http://www.ncbi.nlm.nih.gov/entrez/query.fcgi?cmd=Retrieve&db=PubMed&dopt=Abstract&list_uids=23064518)
Google Scholar (http://scholar.google.com/scholar_lookup?title=High-sensitivity%20Orbitrap%20mass%20analysis%20of%20intact%20macromolecular%20assemblies&author=RJ.%20Rose&author=E.%20Damoc&author=E.%20Denisov&journal=Nat%20Methods&volume=9&pages=1084-1086&publication_year=2012)
29. Ghaemmaghami S, Huh W-K, Bower K et al (2003) Global analysis of protein expression in yeast. *Nature* 425:737–741
PubMed (http://www.ncbi.nlm.nih.gov/entrez/query.fcgi?cmd=Retrieve&db=PubMed&dopt=Abstract&list_uids=14562106)
Google Scholar (http://scholar.google.com/scholar_lookup?title=Global%20analysis%20of%20protein%20expression%20in%20yeast&author=S.%20Ghaemmaghami&author=W-K.%20Huh&author=K.%20Bower&journal=Nature&volume=425&pages=737-741&publication_year=2003)
30. LaCava J, Chandramouli N, Jiang H, Rout MP (2013) Improved native isolation of endogenous protein A-tagged protein complexes. *BioTechniques* 54:213–216
PubMed (http://www.ncbi.nlm.nih.gov/entrez/query.fcgi?cmd=Retrieve&db=PubMed&dopt=Abstract&list_uids=23581468)
PubMedCentral (<http://www.ncbi.nlm.nih.gov/pmc/articles/PMC3667664>)
Google Scholar (http://scholar.google.com/scholar_lookup?title=Improved%20native%20isolation%20of%20endogenous%20protein%20A-tagged%20protein%20complexes&author=J.%20LaCava&author=N.%20Chandramouli&author=H.%20Jiang&author=MP.%20Rout&journal=BioTechniques&volume=54&pages=213-216&publication_year=2013)
31. Cristea IM, Chait BT (2011) Conjugation of magnetic beads for immunopurification of protein complexes. *Cold Spring Harb Protoc* 6:534–538
Google Scholar (http://scholar.google.com/scholar_lookup?title=Conjugation%20of%20magnetic%20beads%20for%20immunopurification%20of%20protein%20complexes&author=IM.%20Cristea&author=BT.%20Chait&journal=Cold%20Spring%20Harb%20Protoc&volume=6&pages=534-538&publication_year=2011)
32. Carrington JC, Dougherty WG (1988) A viral cleavage site cassette: identification of amino acid sequences required for tobacco etch virus polyprotein processing. *Proc Natl Acad Sci U S A* 85:3391–3395
PubMed (http://www.ncbi.nlm.nih.gov/entrez/query.fcgi?cmd=Retrieve&db=PubMed&dopt=Abstract&list_uids=3285343)
PubMedCentral (<http://www.ncbi.nlm.nih.gov/pmc/articles/PMC280215>)
Google Scholar (http://scholar.google.com/scholar_lookup?title=A%20viral%20cleavage%20site%20cassette%3A%20identification%20of%20amino%20acid%20sequences%20required%20for%20tobacco%20etch%20virus%20polyprotein%20processing&author=JC.%20Carrington&author=WG.%20Dougherty&journal=Proc%20Natl%20Acad%20Sci%20U%20S%20A&volume=85&pages=3391-3395&publication_year=1988)
33. Parks TD, Leuther KK, Howard ED et al (1994) Release of proteins and peptides from fusion proteins using a recombinant plant virus proteinase. *Anal Biochem* 216:413–417
PubMed (http://www.ncbi.nlm.nih.gov/entrez/query.fcgi?cmd=Retrieve&db=PubMed&dopt=Abstract&list_uids=8179197)
Google Scholar (http://scholar.google.com/scholar_lookup?title=Release%20of%20proteins%20and%20peptides%20from%20fusion%20proteins%20using%20a%20recombinant%20plant%20virus%20proteinase&author=TD.%20Parks&author=KK.%20Leuther&author=ED.%20Howard&journal=Anal%20Biochem&volume=216&pages=413-417&publication_year=1994)
34. Kapust RB, Toózseór J, Copeland TD, Waugh DS (2002) The P1' specificity of tobacco etch virus protease. *Biochem Biophys Res Commun* 294:949–955
PubMed (http://www.ncbi.nlm.nih.gov/entrez/query.fcgi?cmd=Retrieve&db=PubMed&dopt=Abstract&list_uids=12074568)
Google Scholar (http://scholar.google.com/scholar_lookup?title=The%20P1%E2%80%B2%20specificity%20of%20tobacco%20etch%20virus%20protease&author=RB.%20Kapust&author=J.%20To%20C3%B6zse%C3%B3r&author=TD.%20Copeland&author=DS.%20Waugh&journal=Biochem%20Biophys%20Res%20Commun&volume=294&pages=949-955&publication_year=2002)
35. Wilm M, Mann M (1996) Analytical properties of the nanoelectrospray ion source. *Anal Chem* 68:1–8
PubMed (http://www.ncbi.nlm.nih.gov/entrez/query.fcgi?cmd=Retrieve&db=PubMed&dopt=Abstract&list_uids=8779426)
Google Scholar (http://scholar.google.com/scholar_lookup?title=Analytical%20properties%20of%20the%20nanoelectrospray%20ion%20source&author=M.%20Wilm&author=M.%20Mann&journal=Anal%20Chem&volume=68&pages=1-8&publication_year=1996)
36. Lössl P, Snijder J, Heck AJR (2014) Boundaries of mass resolution in native mass spectrometry. *J Am Soc Mass Spectrom* 25:906–917
PubMed (http://www.ncbi.nlm.nih.gov/entrez/query.fcgi?cmd=Retrieve&db=PubMed&dopt=Abstract&list_uids=24700121)
Google Scholar (http://scholar.google.com/scholar_lookup?title=Boundaries%20of%20mass%20resolution%20in%20native%20mass%20spectrometry&author=P.%20L%C3%B6ssl&author=J.%20Snijder&author=AJR.%20Heck&journal=J%20Am%20Soc%20Mass%20Spectrom&volume=25&pages=906-917&publication_year=2014)
37. Marty MT, Baldwin AJ, Marklund EG et al (2015) Bayesian Deconvolution of mass and ion mobility spectra:

- from binary interactions to Polydisperse ensembles. *Anal Chem* 87:4370–4376
[PubMed](http://www.ncbi.nlm.nih.gov/entrez/query.fcgi?cmd=Retrieve&db=PubMed&dopt=Abstract&list_uids=25799115) (http://www.ncbi.nlm.nih.gov/entrez/query.fcgi?cmd=Retrieve&db=PubMed&dopt=Abstract&list_uids=25799115)
[PubMedCentral](http://www.ncbi.nlm.nih.gov/pmc/articles/PMC4594776) (http://www.ncbi.nlm.nih.gov/pmc/articles/PMC4594776)
[Google Scholar](http://scholar.google.com/scholar_lookup?title=Bayesian%20Deconvolution%20of%20mass%20and%20ion%20mobility%20spectra%3A%20from%20binary%20interactions%20to%20Polydisperse%20ensembles&author=MT.%20Marty&author=AJ.%20Baldwin&author=EG.%20Marklund&journal=Anal%20Chem&volume=87&pages=4370-4376&publication_year=2015) (http://scholar.google.com/scholar_lookup?title=Bayesian%20Deconvolution%20of%20mass%20and%20ion%20mobility%20spectra%3A%20from%20binary%20interactions%20to%20Polydisperse%20ensembles&author=MT.%20Marty&author=AJ.%20Baldwin&author=EG.%20Marklund&journal=Anal%20Chem&volume=87&pages=4370-4376&publication_year=2015)
38. Reid DJ, Dising JM, Miller MA et al (2019) MetaUniDec: high-throughput deconvolution of native mass spectra. *J Am Soc Mass Spectrom* 30:118–127
[Google Scholar](https://scholar.google.com/scholar?q=Reid%20DJ%20Dising%20JM%20Miller%20MA%20et%20al%20%282019%29%20MetaUniDec%3A%20high-throughput%20deconvolution%20of%20native%20mass%20spectra.%20J%20Am%20Soc%20Mass%20Spectrom%2030%3A118%E2%80%93127) (https://scholar.google.com/scholar?q=Reid%20DJ%20Dising%20JM%20Miller%20MA%20et%20al%20%282019%29%20MetaUniDec%3A%20high-throughput%20deconvolution%20of%20native%20mass%20spectra.%20J%20Am%20Soc%20Mass%20Spectrom%2030%3A118%E2%80%93127)
39. Sobott F, Hernández H, McCammon MG et al (2002) A tandem mass spectrometer for improved transmission and analysis of large macromolecular assemblies. *Anal Chem* 74:1402–1407
[PubMed](http://www.ncbi.nlm.nih.gov/entrez/query.fcgi?cmd=Retrieve&db=PubMed&dopt=Abstract&list_uids=11922310) (http://www.ncbi.nlm.nih.gov/entrez/query.fcgi?cmd=Retrieve&db=PubMed&dopt=Abstract&list_uids=11922310)
[Google Scholar](http://scholar.google.com/scholar_lookup?title=A%20tandem%20mass%20spectrometer%20for%20improved%20transmission%20and%20analysis%20of%20large%20macromolecular%20assemblies&author=F.%20Sobott&author=H.%20Hern%C3%A1ndez&author=MG.%20McCammon&journal=Anal%20Chem&volume=74&pages=1402-1407&publication_year=2002) (http://scholar.google.com/scholar_lookup?title=A%20tandem%20mass%20spectrometer%20for%20improved%20transmission%20and%20analysis%20of%20large%20macromolecular%20assemblies&author=F.%20Sobott&author=H.%20Hern%C3%A1ndez&author=MG.%20McCammon&journal=Anal%20Chem&volume=74&pages=1402-1407&publication_year=2002)
40. Van Den Heuvel RHH, Van Duijn E, Mazon H et al (2006) Improving the performance of a quadrupole time-of-flight instrument for macromolecular mass spectrometry. *Anal Chem* 78:7473–7483
[PubMed](http://www.ncbi.nlm.nih.gov/entrez/query.fcgi?cmd=Retrieve&db=PubMed&dopt=Abstract&list_uids=17073415) (http://www.ncbi.nlm.nih.gov/entrez/query.fcgi?cmd=Retrieve&db=PubMed&dopt=Abstract&list_uids=17073415)
[Google Scholar](http://scholar.google.com/scholar_lookup?title=Improving%20the%20performance%20of%20a%20quadrupole%20time-of-flight%20instrument%20for%20macromolecular%20mass%20spectrometry&author=RHH.%20Heuvel&author=E.%20Duijn&author=H.%20Mazon&journal=Anal%20Chem&volume=78&pages=7473-7483&publication_year=2006) (http://scholar.google.com/scholar_lookup?title=Improving%20the%20performance%20of%20a%20quadrupole%20time-of-flight%20instrument%20for%20macromolecular%20mass%20spectrometry&author=RHH.%20Heuvel&author=E.%20Duijn&author=H.%20Mazon&journal=Anal%20Chem&volume=78&pages=7473-7483&publication_year=2006)
41. Pringle SD, Giles K, Wildgoose JL et al (2007) An investigation of the mobility separation of some peptide and protein ions using a new hybrid quadrupole/travelling wave IMS/oa-ToF instrument. *Int J Mass Spectrom* 261:1–12
[Google Scholar](http://scholar.google.com/scholar_lookup?title=An%20investigation%20of%20the%20mobility%20separation%20of%20some%20peptide%20and%20protein%20ions%20using%20a%20new%20hybrid%20quadrupole%20travelling%20wave%20IMS%20Foa-ToF%20instrument&author=SD.%20Pringle&author=K.%20Giles&author=JL.%20Wildgoose&journal=Int%20J%20Mass%20Spectrom&volume=261&pages=1-12&publication_year=2007) (http://scholar.google.com/scholar_lookup?title=An%20investigation%20of%20the%20mobility%20separation%20of%20some%20peptide%20and%20protein%20ions%20using%20a%20new%20hybrid%20quadrupole%20travelling%20wave%20IMS%20Foa-ToF%20instrument&author=SD.%20Pringle&author=K.%20Giles&author=JL.%20Wildgoose&journal=Int%20J%20Mass%20Spectrom&volume=261&pages=1-12&publication_year=2007)
42. Hernández H, Robinson CV (2007) Determining the stoichiometry and interactions of macromolecular assemblies from mass spectrometry. *Nat Protoc* 2:715–726
[PubMed](http://www.ncbi.nlm.nih.gov/entrez/query.fcgi?cmd=Retrieve&db=PubMed&dopt=Abstract&list_uids=17406634) (http://www.ncbi.nlm.nih.gov/entrez/query.fcgi?cmd=Retrieve&db=PubMed&dopt=Abstract&list_uids=17406634)
[Google Scholar](http://scholar.google.com/scholar_lookup?title=Determining%20the%20stoichiometry%20and%20interactions%20of%20macromolecular%20assemblies%20from%20mass%20spectrometry&author=H.%20Hern%C3%A1ndez&author=CV.%20Robinson&journal=Nat%20Protoc&volume=2&pages=715-726&publication_year=2007) (http://scholar.google.com/scholar_lookup?title=Determining%20the%20stoichiometry%20and%20interactions%20of%20macromolecular%20assemblies%20from%20mass%20spectrometry&author=H.%20Hern%C3%A1ndez&author=CV.%20Robinson&journal=Nat%20Protoc&volume=2&pages=715-726&publication_year=2007)
43. Kondrat FDL, Struwe WB, Benesch JLP (2015) Native mass spectrometry: towards high-throughput structural proteomics. *Methods Mol Biol* 1261:349–371
[PubMed](http://www.ncbi.nlm.nih.gov/entrez/query.fcgi?cmd=Retrieve&db=PubMed&dopt=Abstract&list_uids=25502208) (http://www.ncbi.nlm.nih.gov/entrez/query.fcgi?cmd=Retrieve&db=PubMed&dopt=Abstract&list_uids=25502208)
[Google Scholar](http://scholar.google.com/scholar_lookup?title=Native%20mass%20spectrometry%3A%20towards%20high-throughput%20structural%20proteomics&author=FDL.%20Kondrat&author=WB.%20Struwe&author=JLP.%20Benesch&journal=Methods%20Mol%20Biol&volume=1261&pages=349-371&publication_year=2015) (http://scholar.google.com/scholar_lookup?title=Native%20mass%20spectrometry%3A%20towards%20high-throughput%20structural%20proteomics&author=FDL.%20Kondrat&author=WB.%20Struwe&author=JLP.%20Benesch&journal=Methods%20Mol%20Biol&volume=1261&pages=349-371&publication_year=2015)
44. Belov ME, Damoc E, Denisov E et al (2013) From protein complexes to subunit backbone fragments: a multi-stage approach to native mass spectrometry. *Anal Chem* 85:11163–11173
[PubMed](http://www.ncbi.nlm.nih.gov/entrez/query.fcgi?cmd=Retrieve&db=PubMed&dopt=Abstract&list_uids=24237199) (http://www.ncbi.nlm.nih.gov/entrez/query.fcgi?cmd=Retrieve&db=PubMed&dopt=Abstract&list_uids=24237199)
[Google Scholar](http://scholar.google.com/scholar_lookup?title=From%20protein%20complexes%20to%20subunit%20backbone%20fragments%3A%20a%20multi-stage%20approach%20to%20native%20mass%20spectrometry&author=ME.%20Belov&author=E.%20Damoc&author=E.%20Denisov&journal=Anal%20Chem&volume=85&pages=11163-11173&publication_year=2013) (http://scholar.google.com/scholar_lookup?title=From%20protein%20complexes%20to%20subunit%20backbone%20fragments%3A%20a%20multi-stage%20approach%20to%20native%20mass%20spectrometry&author=ME.%20Belov&author=E.%20Damoc&author=E.%20Denisov&journal=Anal%20Chem&volume=85&pages=11163-11173&publication_year=2013)
45. Ben-Nissan G, Belov ME, Morgenstern D et al (2017) Triple-stage mass spectrometry unravels the heterogeneity of an endogenous protein complex. *Anal Chem* 89:4708–4715
[PubMed](http://www.ncbi.nlm.nih.gov/entrez/query.fcgi?cmd=Retrieve&db=PubMed&dopt=Abstract&list_uids=28345864) (http://www.ncbi.nlm.nih.gov/entrez/query.fcgi?cmd=Retrieve&db=PubMed&dopt=Abstract&list_uids=28345864)
[PubMedCentral](http://www.ncbi.nlm.nih.gov/pmc/articles/PMC5702261) (http://www.ncbi.nlm.nih.gov/pmc/articles/PMC5702261)
[Google Scholar](http://scholar.google.com/scholar_lookup?title=Triple-stage%20mass%20spectrometry%20unravels%20the%20heterogeneity%20of%20an%20endogenous%20protein%20complex&author=G.%20Ben-Nissan&author=ME.%20Belov&author=D.%20Morgenstern&journal=Anal%20Chem&volume=89&pages=4708) (http://scholar.google.com/scholar_lookup?title=Triple-stage%20mass%20spectrometry%20unravels%20the%20heterogeneity%20of%20an%20endogenous%20protein%20complex&author=G.%20Ben-Nissan&author=ME.%20Belov&author=D.%20Morgenstern&journal=Anal%20Chem&volume=89&pages=4708)

-4715&publication_year=2017)

46. van de Waterbeemd M, Fort KL, Boll D et al (2017) High-fidelity mass analysis unveils heterogeneity in intact ribosomal particles. *Nat Methods* 14:283–286
PubMed (http://www.ncbi.nlm.nih.gov/entrez/query.fcgi?cmd=Retrieve&db=PubMed&dopt=Abstract&list_uids=28114288)
Google Scholar (http://scholar.google.com/scholar_lookup?title=High-fidelity%20mass%20analysis%20unveils%20heterogeneity%20in%20intact%20ribosomal%20particles&author=M.%20Waterbeemd&author=KL.%20Fort&author=D.%20Boll&journal=Nat%20Methods&volume=14&pages=283-286&publication_year=2017)
47. Makarov A (2000) Electrostatic axially harmonic orbital trapping: a high-performance technique of mass analysis. *Anal Chem* 72:1156–1162
PubMed (http://www.ncbi.nlm.nih.gov/entrez/query.fcgi?cmd=Retrieve&db=PubMed&dopt=Abstract&list_uids=10740853)
Google Scholar (http://scholar.google.com/scholar_lookup?title=Electrostatic%20axially%20harmonic%20orbital%20trapping%3A%20a%20high-performance%20technique%20of%20mass%20analysis&author=A.%20Makarov&journal=Anal%20Chem&volume=72&pages=1156-1162&publication_year=2000)
48. Makarov A, Denisov E (2009) Dynamics of ions of intact proteins in the orbitrap mass analyzer. *J Am Soc Mass Spectrom* 20:1486–1495
PubMed (http://www.ncbi.nlm.nih.gov/entrez/query.fcgi?cmd=Retrieve&db=PubMed&dopt=Abstract&list_uids=19427230)
Google Scholar (http://scholar.google.com/scholar_lookup?title=Dynamics%20of%20ions%20of%20intact%20proteins%20in%20the%20orbitrap%20mass%20analyzer&author=A.%20Makarov&author=E.%20Denisov&journal=J%20Am%20Soc%20Mass%20Spectrom&volume=20&pages=1486-1495&publication_year=2009)
49. Benesch JLP, Aquilina JA, Ruotolo BT et al (2006) Tandem mass spectrometry reveals the quaternary organization of macromolecular assemblies. *Chem Biol* 13:597–605
PubMed (http://www.ncbi.nlm.nih.gov/entrez/query.fcgi?cmd=Retrieve&db=PubMed&dopt=Abstract&list_uids=16793517)
Google Scholar (http://scholar.google.com/scholar_lookup?title=Tandem%20mass%20spectrometry%20reveals%20the%20quaternary%20organization%20of%20macromolecular%20assemblies&author=JLP.%20Benesch&author=JA.%20Aquilina&author=BT.%20Ruotolo&journal=Chem%20Biol&volume=13&pages=597-605&publication_year=2006)
50. Makino DL, Baumgärtner M, Conti E (2013) Crystal structure of an RNA-bound 11-subunit eukaryotic exosome complex. *Nature* 495:70–75
PubMed (http://www.ncbi.nlm.nih.gov/entrez/query.fcgi?cmd=Retrieve&db=PubMed&dopt=Abstract&list_uids=23376952)
Google Scholar (http://scholar.google.com/scholar_lookup?title=Crystal%20structure%20of%20an%20RNA-bound%2011-subunit%20eukaryotic%20exosome%20complex&author=DL.%20Makino&author=M.%20Baumg%C3%A4rtner&author=E.%20Conti&journal=Nature&volume=495&pages=70-75&publication_year=2013)

Copyright information

© Springer Science+Business Media, LLC, part of Springer
Nature 2020

About this protocol

Cite this protocol as:

Olinares P.D.B., Chait B.T. (2020) Native Mass Spectrometry Analysis of Affinity-Captured Endogenous Yeast RNA Exosome Complexes. In: LaCava J., Vaňáčková Š. (eds) The Eukaryotic RNA Exosome. *Methods in Molecular Biology*, vol 2062. Humana, New York, NY. https://doi.org/10.1007/978-1-4939-9822-7_17

First Online

26 November 2019

DOI

https://doi.org/10.1007/978-1-4939-9822-7_17

Publisher Name

Humana, New York, NY

Print ISBN

978-1-4939-9821-0

Online ISBN

978-1-4939-9822-7

eBook Packages

[Springer Protocols](#)

[Reprints and Permissions](#)

SPRINGER NATURE

© 2020 Springer Nature Switzerland AG. Part of [Springer Nature](#).

Not logged in · The Rockefeller University (1600185088) - LYRASIS (3000176756) - The Rockefeller University Library (8200893941) · 129.85.225.78